

NRAP reduction rescues sarcomere defects in nebulin-related nemaline myopathy

Jennifer G. Casey¹, Euri S. Kim¹, Remi Joseph¹, Frank Li², Henk Granzier² and Vandana A. Gupta^{1,*}

¹Division of Genetics, Department of Medicine, Brigham and Women's Hospital, Harvard Medical School, Boston, MA 02115, USA

²Department of Cellular and Molecular Medicine, University of Arizona, Tucson, AZ 85724, USA

*To whom correspondence should be addressed at: Vandana A. Gupta, Division of Genetics, Department of Medicine, Brigham and Women's Hospital, Harvard Medical School, Boston, MA 02115, USA. Email: vgupta@research.bwh.harvard.edu

Abstract

Nemaline myopathy (NM) is a rare neuromuscular disorder associated with congenital or childhood-onset of skeletal muscle weakness and hypotonia, which results in limited motor function. NM is a genetic disorder and mutations in 12 genes are known to contribute to autosomal dominant or recessive forms of the disease. Recessive mutations in nebulin (*NEB*) are the most common cause of NM affecting about 50% of patients. Because of the large size of the *NEB* gene and lack of mutational hot spots, developing therapies that can benefit a wide group of patients is challenging. Although there are several promising therapies under investigation, there is no cure for NM. Therefore, targeting disease modifiers that can stabilize or improve skeletal muscle function may represent alternative therapeutic strategies. Our studies have identified Nrap upregulation in nebulin deficiency that contributes to structural and functional deficits in NM. We show that genetic ablation of *nrap* in nebulin deficiency restored sarcomeric disorganization, reduced protein aggregates and improved skeletal muscle function in zebrafish. Our findings suggest that Nrap is a disease modifier that affects skeletal muscle structure and function in NM; thus, therapeutic targeting of Nrap in nebulin-related NM and related diseases may be beneficial for patients.

Introduction

Nemaline myopathy (NM) is a common form of congenital myopathy, affecting approximately 1 in 50 000 individuals (1,2). NM is a clinically heterogeneous disorder ranging from severe neonatal presentations to a milder onset in late childhood or adult stage. The disease is characterized by generalized muscle weakness and the presence of protein aggregates in skeletal muscle (nemaline bodies). Genetically, NM is caused by mutations in 12 genes that encode either structural proteins that constitute the thin filaments in the sarcomere or proteins that regulate the formation and maintenance of thin filaments (3–13). The most common form of NM is caused by recessive mutations in *NEB*, encoding nebulin protein (4).

Most mutations identified to date in *NEB* result in frameshift, premature stop codons or splicing changes, causing truncations or deletions within the protein (7,14,15). Missense variants are common in *NEB* but are difficult to validate functionally because of the large size of nebulin. Mutations in *NEB* are distributed throughout the gene, and, to date, no mutation hotspots have been discovered other than a founder mutation in individuals of Ashkenazi Jewish ancestry. This mutation results in the deletion of the entire exon 55 of *NEB*, which leads to an in-frame deletion of 35 amino acids, likely disturbing the super-repeat structure of the protein (16). The nebulin gene (*NEB*) comprises 183 exons spanning 249 kb of genomic sequence and 20.8 kb of the cDNA sequence (17). Nebulin transcripts are extensively spliced depending on the muscle type and developmental stage (18). Frequently, multiple isoforms are also present at the same time. The nebulin protein consists mostly of repeat modules of 35–40 residues

containing an SDXXYK motif, called simple repeats (19). Depending on the splice isoform, the number of simple repeats varies from 179 to 239 (20). The central part of the nebulin is organized into super-repeats made up of seven simple repeats each and contains a conserved WLKIGW motif and nebulin proteins with different numbers of super repeats are expressed within the same muscle regardless of muscle types (17,21). This change in length is further complicated by copy number variation in the triplicate region of *NEB* (22). The N- and C-terminus domains of nebulin are not organized into super-repeats but have specific domains and sequences that interact with different proteins in the skeletal muscle to stabilize the sarcomere structure and are critical for their function (19).

The function of nebulin is highly conserved in vertebrates. *Neb* knockout mice recapitulate the congenital form of NM with misaligned myofibrils, formation of nemaline bodies and severe muscle weakness and die at 8–10 days after birth (23–25). Mouse models lacking specific nebulin domains or modeling missense mutations in nebulin exhibit a mild or moderate muscle phenotype similar to NM patients (26–30). *neb* KO zebrafish also exhibit altered sarcomere structure and muscle weakness with nemaline bodies (31). Thus, animal models that express mutant nebulin or completely lack nebulin reflect the skeletal muscle pathology of human NM and provide an excellent system for preclinical therapeutic developments.

Currently, there are no therapies available for NM. Therapeutic developments for nebulin are particularly challenging because of the large size of the gene, extensive alternative splicing events that are poorly understood and lack of hot spot mutation regions.

This limits the application of recently successful approaches such as gene therapy and CRISPR-based gene editing approaches to develop therapies for nebulin deficient NM. Previously, our work has identified that upregulation of Nrap in skeletal muscle contributes to disease pathology. Downregulation of Nrap improved the skeletal muscle structure and function in KLHL41-NM (32). Our current studies identified abnormal upregulation of Nrap levels in nebulin mutant mice and zebrafish animal models. We further show that the genetic downregulation of *nrap* in nebulin deficient zebrafish improved the structure and function of skeletal muscle and increased the lifespan of *neb* mutant larval zebrafish. This work identified Nrap reduction as an effective therapeutic approach in preclinical studies and opened new therapeutic avenues for NEB-NM.

Results

Nrap is upregulated in nebulin deficiency

NRAP is a nebulin family member that is highly expressed in skeletal muscle during embryonic development and exhibits low expression in the post-natal muscle (33). In many disease states such as nemaline and myofibrillar myopathy, increased levels of NRAP are detected in the post-natal skeletal muscle (32,34). Our previous studies have shown that overexpression of NRAP in skeletal muscle results in myopathic phenotypes in zebrafish and that downregulation of Nrap improved the structure and function of skeletal muscle in KLHL41-NM (32). Therefore, to investigate NRAP as a therapeutic target in nebulin-NM, we evaluated *nrap* mRNA and protein expression in nebulin mutant mice and zebrafish. These animal models recapitulate the disease pathology similar to NM patients (28,31,35). Western blotting analysis of different skeletal muscle types in control and *Neb* mutant mice (*Neb* $\Delta^{163-165}$) identified a significant increase in NRAP protein in nebulin deficiency in mice (Fig. 1A–B). Previous studies have also shown increased levels of *Nrap* mRNA in *Neb* mutant mice (*Neb* $\Delta^{163-165}$) (36). RT-PCR analysis in *neb* $-/-$ zebrafish (*neb*⁹⁰⁶, obtained from Zebrafish International Resource Center, ZIRC) (35) also showed an increase in *nrap* transcripts in *neb* $-/-$ fish compared with controls (Fig. 1C and E). Similarly, Western blot analysis in control and *neb* $-/-$ zebrafish (6 dpf) identified a significant increase in Nrap protein levels in the *neb* $-/-$ fish in comparison with wild-type siblings (controls) (Fig. 1D and F). These studies show that increased NRAP levels are associated with nebulin deficiency in vertebrate NM animal models.

Abnormal subcellular changes in nrap localization in nebulin deficiency

To understand if increased levels of Nrap protein in nebulin deficiency are associated with any changes in the subcellular localization, immunofluorescence was performed on myofibers isolated from control and *neb* $-/-$ zebrafish at 6 dpf. NRAP protein is localized at myofiber ends at myotendinous junctions (MTJ) in mice skeletal muscle (36–39). Similar to mice, Nrap localization was observed at myofiber ends in control zebrafish myofibers (Fig. 2A) (40). In contrast, Nrap was randomly localized in different regions of the myofibers in *neb* $-/-$ zebrafish (Fig. 2A). This abnormal localization of Nrap was observed in myofibers with different levels of thin filament defects detected by reduced or lack of phalloidin staining (Fig. 2A). *neb* $-/-$ myofibers also displayed increased immunoreactivity for Nrap protein at the myofiber ends compared with controls. Therefore, increased Nrap protein in *neb* $-/-$ mutant myofibers is present at MTJs where Nrap is normally localized, as well as in random distribution throughout

the myofibers. Quantification of the fractional area of myofibers exhibiting abnormal Nrap localization showed a large variability between individual myofibers (18–46%) (Fig. 2B). This abnormal Nrap localization was observed in most myofibers examined in *neb* $-/-$ zebrafish ($82 \pm 7.2\%$) compared with controls (Fig. 2C). In NM, nemaline bodies or protein aggregates in skeletal muscle contain sarcomeric α -actinin protein. To evaluate if abnormal Nrap observed in *neb* $-/-$ myofibers overlaps with sarcomeric protein aggregates or nemaline bodies usually present in nebulin deficient muscle, Nrap coimmunofluorescence was performed with sarcomeric α -actinin and actin. Co-immunofluorescence showed partial co-localization of Nrap with sarcomeric α -actinin (Actn2/3) at myofiber ends. These studies suggest that in the absence of nebulin, an increased amount of Nrap exhibits abnormal mislocalization in myofibers and partially co-localizes with the sarcomeric protein aggregates present in the *neb* $-/-$ myofibers.

Nrap deficient zebrafish exhibit normal skeletal muscle and cardiac function

Our previous studies have shown that overexpression of NRAP in skeletal muscle results in myopathy in transgenic zebrafish (32). This suggests that a reduction of abnormally increased amounts of Nrap in nebulin deficient skeletal muscle may improve the structural and functional defects associated with nebulin deficiency. Before testing Nrap downregulation as a potential therapy, we first examined the effect of loss of *nrap* on skeletal and cardiac muscle function in the *nrap* zebrafish line (*nrap*^{sa42059}, obtained from ZIRC). To evaluate the effect of Nrap reduction in skeletal muscle, wild-type (control), *nrap* $+/-$ and *nrap* $-/-$ siblings were examined. Phenotypic analysis showed no obvious differences between control and *nrap* $-/-$ larval fish (3 dpf) (Fig. 3A, left panel). Birefringence analysis was performed to examine skeletal muscle organization which also showed no differences in the birefringence between control and *nrap* $-/-$ fish (Fig. 3A–B, right panel). Control and *nrap* $-/-$ embryonic and larval fish exhibited the expected Mendelian ratio (0 dpf – 12 months examined), suggesting Nrap deficiency does not result in lethality at embryonic or adult stages (Fig. 3C). Cardiac function was also analyzed in control and *nrap* $-/-$ larval fish (7 dpf) by examining the heart rate, which showed no significant difference between these two groups (Fig. 3D). These analyses show that loss of *nrap* does not affect survival and/or skeletal and cardiac muscle function in zebrafish.

Nrap downregulation improves swim performance and survival in *neb* zebrafish

To determine whether reducing abnormal Nrap levels may rescue NM because of *Neb* deficiency, Nrap was reduced in the *neb* $-/-$ fish at the genetic level by crossing *neb* and *nrap* zebrafish lines. *Neb* $+/-$ zebrafish were crossed with *nrap* $+/-$ zebrafish to obtain *neb* $+/-nrap $+/-$ double heterozygote line that was further crossed to obtain *neb* $-/-nrap $+/-$ and *neb* $-/-nrap $-/-$ embryos. To evaluate the effect of *nrap* downregulation, wild-type controls, *neb* $-/-$, *nrap* $-/-$, *neb* $-/-nrap $+/-$ and *neb* $-/-nrap $-/-$ sibling groups were analyzed for survival and skeletal muscle function. *Neb* $-/-$ mutant zebrafish larvae start to exhibit lethality from 5 dpf and 100% *neb* $-/-$ mutant zebrafish larvae die by 7 dpf. 50% reduction of Nrap in *neb* $-/-nrap $+/-$ larval fish significantly increased survival from 5 dpf onwards to 12 dpf compared with *neb* $-/-$ zebrafish. A complete absence of Nrap in *neb* $-/-nrap $-/-$ zebrafish also resulted in an improved survival from 6 dpf to 10 dpf compared with *neb* $-/-$ zebrafish (Fig. 4A). To analyze if the Nrap downregulation also improves skeletal muscle function,$$$$$$$

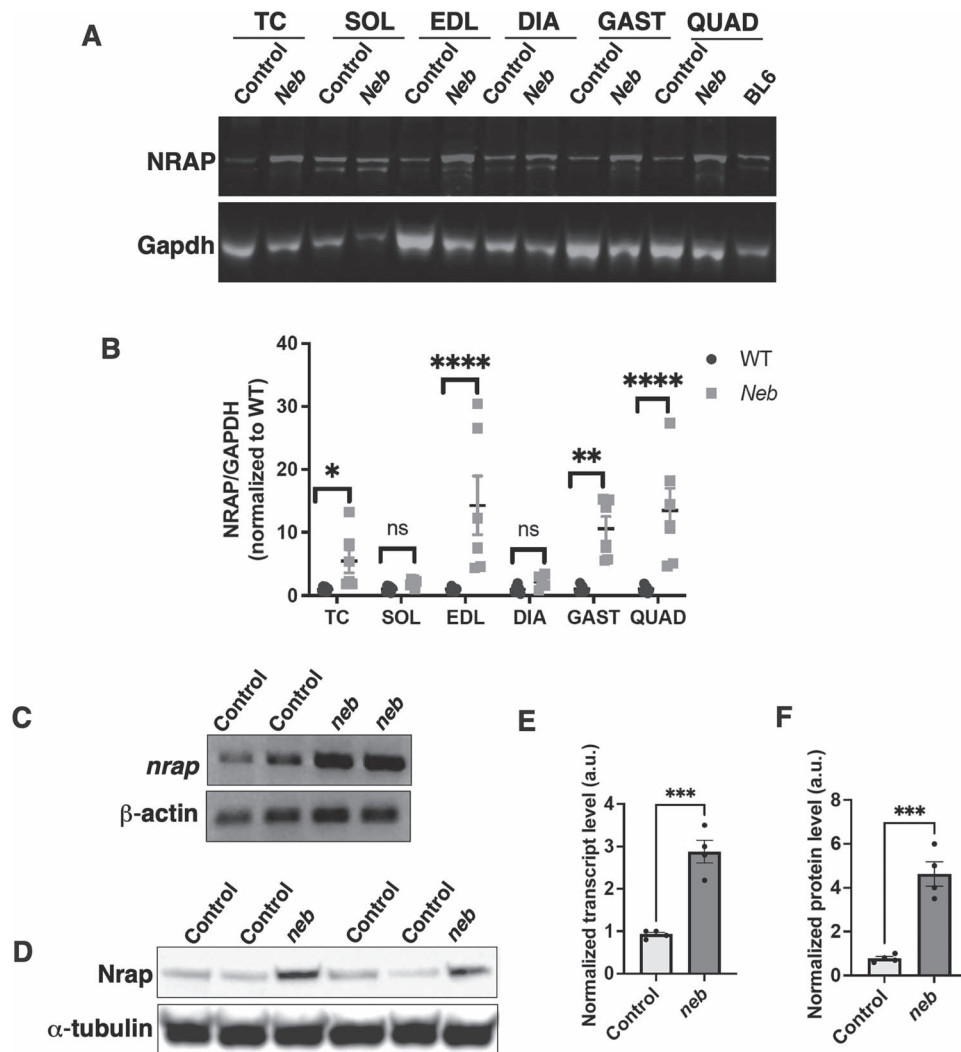


Figure 1. NRAP is upregulated in nebulin deficiency in zebrafish and mice skeletal muscle. (A) Western blot of proteins from different skeletal muscle types in control and *Neb* mutant mice (*Neb* $\Delta^{163-165}$) at 6 weeks. (B) Quantification of NRAP protein in control and (*Neb* $\Delta^{163-165}$) at 6 weeks. (C) RT-PCR analysis of mRNA in control and *neb* mutant fish (7 dpf). (D) Western blot of proteins from control and *neb* mutant zebrafish (7 dpf). (E–F). Quantification of *nrp* mRNA and protein in control and *neb* mutant fish (7 dpf), respectively. Data represent mean \pm SD from three different experiments. Non-significant: ns, * $p < 0.05$, ** $p < 0.01$, *** $p < 0.001$, **** $p < 0.0001$, Student's *t* test. Number of mice in (A) and (B): WT: 3, mutant: 6. Number of zebrafish in (C) and (D): 25–40 in each group.

automated swimming behavior was analyzed by tracking individual fish in the multiwell format and total distance was quantified. *Neb* $^{-/-}$ *nrp* $^{+/-}$ zebrafish larvae swam to a significantly higher distance compared with *neb* $^{-/-}$ zebrafish at 6 dpf that are mostly immobile at this stage (Fig. 4B). *neb* $^{-/-}$ *nrp* $^{-/-}$ zebrafish also showed significantly improved swimming behavior in comparison to *neb* $^{-/-}$ fish but to a lesser extent than *neb* $^{-/-}$ *nrp* $^{+/-}$ fish. These results demonstrate that *Nrap* reduction improves the survival and swimming performance of *Neb* deficient zebrafish.

***Nrap* downregulation improves skeletal muscle organization and reduces protein aggregates in myofibers**

Nebulin deficiency results in hypotonia, disorganized myofibers and the presence of protein aggregates (nemaline bodies) in patients and animal models. To analyze the effect of *Nrap* modulation on myotome organization in zebrafish, whole mount immunofluorescence with phalloidin was performed

on larval zebrafish (6 dpf). *neb* $^{-/-}$ zebrafish exhibited disorganized myotome and the presence of actin aggregates in the myofibers as reported previously in *neb* $^{-/-}$ zebrafish models (Fig. 5A). The number of sarcomeres in each myofiber was also significantly reduced in *neb* $^{-/-}$ fish compared with wild-type siblings (controls) (Fig. 5A–B). Clinically, many patients with *NEB* mutations exhibit contractures of the upper and lower extremities (41). Although the exact mechanism of contractures is still not clear, a decrease in sarcomeres in series has been shown to contribute to contractures (42). This indicates nebulin deficiency in zebrafish also results in contractures similar to nemaline patients. *Nrap* $^{-/-}$ mutant muscle showed normal skeletal muscle organization and sarcomere number compared with wild-type controls. A 50% reduction of *Nrap* in *neb* $^{-/-}$ *nrp* $^{+/-}$ zebrafish resulted in a significant improvement in myofiber organization and a reduction in protein aggregates in myofibers (Fig. 5A–C). The number of sarcomeres per myofiber also showed an increase in *neb* $^{-/-}$ *nrp* $^{+/-}$ zebrafish compared with *neb* $^{-/-}$. The complete absence of *Nrap* in *neb* $^{-/-}$ *nrp* $^{-/-}$ also improved the myofiber organization and resulted in a reduced number

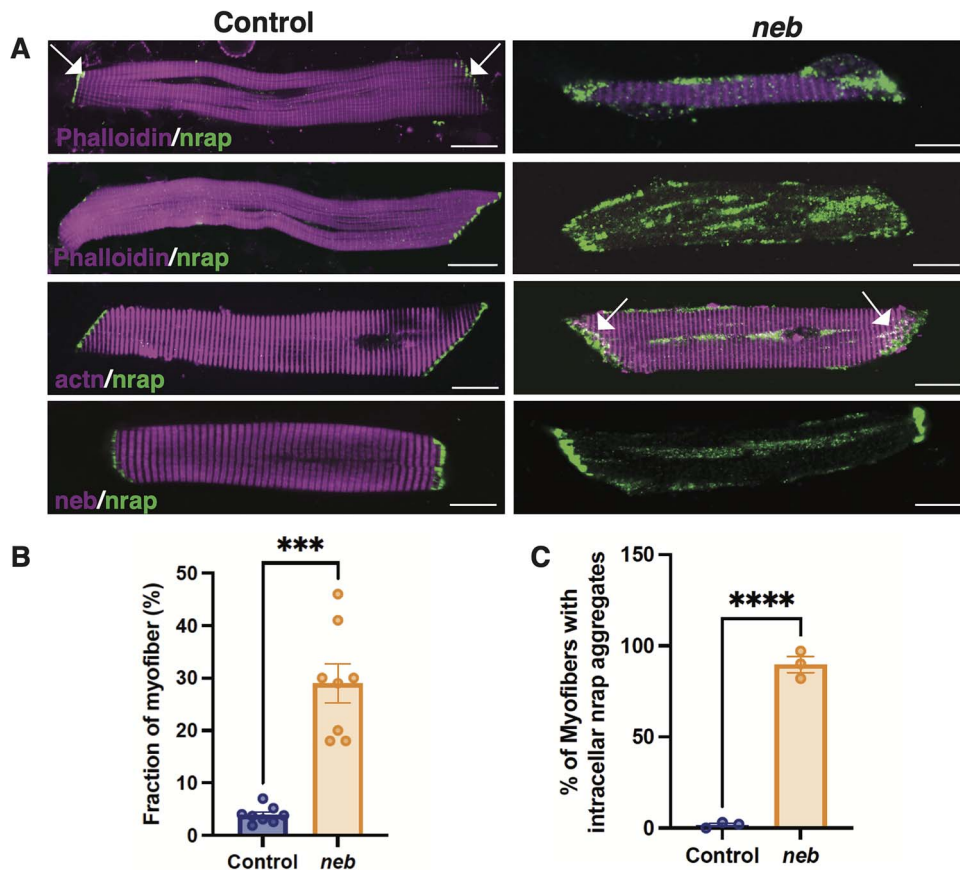


Figure 2. Nrap is mislocalized in myofibers in nebulin deficiency. **(A)** Immunofluorescence of myofibers isolated and cultured from control and *neb*^{-/-} zebrafish (6 dpf) with Nrap and sarcomeric proteins. **(B)** Quantification of myofibers that exhibited intracellular Nrap aggregates. **(C)** Quantification of the fractional area of myofibers exhibiting Nrap immunoreactivity. Unpaired, two-tailed, t test was performed. ****p* < 0.001, *****p* < 0.0001. *n* = 15–30 pooled fish in each group. In all, 15–20 myofibers were analyzed in each group. All images are representative of the *n* = 3 replicates. Bar = 10 μm.

of protein aggregates. Although myotome organization was improved and sarcomeric protein aggregates were reduced on *nrap* downregulation, no significant changes in sarcomere numbers per myofiber were observed in *neb*^{-/-}*nrap*^{-/-} in comparison with *neb*^{-/-} zebrafish (Fig. 5A–B). This suggests that partial *nrap* downregulation improves myotome organization and sarcomere number and reduces the accumulation of protein aggregates in nebulin deficiency.

Nrap downregulation improves sarcomere size, number and organization

The effect of Nrap downregulation on sarcomere structure and organization was further evaluated by examining the ultrastructure of control, *neb*^{-/-}, *nrap*^{-/-}, *neb*^{-/-}*nrap*^{+/-} and *neb*^{-/-}*nrap*^{-/-} sibling groups at 6 dpf (Fig. 6). *neb*^{-/-} zebrafish exhibited reduced sarcomere height (510 ± 107 nm) in comparison to the control sibling (755 ± 192 nm) (Fig. 6A). Interestingly, skeletal muscle in *neb*^{-/-} showed a slight but significant increase in sarcomere length (1475 ± 55 nm) compared with controls (1400 ± 96 nm) (Fig. 6A–B). This slight increase in sarcomere width is consistent with the reduced sarcomere number observed in *neb*^{-/-} zebrafish. *Neb*^{-/-} fish also exhibited the presence of nemaline bodies in the sarcomere (Fig. 6A). Nebulin deficient sarcomeres exhibited an increase in Z band length (Supplementary Material, Fig. S1A). Many sarcomeres also exhibited a lack of Z-lines and an accumulation of membranes

between adjacent myofibrils (Fig. 6A). Nebulin deficient fish also showed an increase in the ratio of I- to A-band length compared with controls indicating a defect in the Z band and thin filaments' length (Supplementary Material, Fig. S1B). No significant ultrastructural changes were observed in *nrap*^{-/-} zebrafish in comparison to controls. Examination of *neb*^{-/-}*nrap*^{-/-} revealed an improvement of sarcomere organization. Z-lines were observed in all the sarcomeres and Z-band length was significantly reduced compared with *neb*^{-/-} fish. Similarly, the I- to A-band length ratio was also reduced compared with *neb*^{-/-} fish (Supplementary Material, Fig. S1). Nemaline bodies were also rarely observed in the skeletal muscle of *neb*^{-/-}*nrap*^{-/-} zebrafish. However, abnormal membrane accumulation between myofibrils was still present as seen in *neb*^{-/-}*nrap*^{-/-} fish. *Neb*^{-/-}*nrap*^{+/-} zebrafish exhibited improved organization of sarcomere with the presence of Z-lines and a reduction in the abnormal membrane accumulation between myofibrils. The Z-band length was significantly decreased compared with *neb*^{-/-} fish. I- to A-band length ratio was also reduced in comparison to *neb*^{-/-} fish (Supplementary Material, Fig. S1). No nemaline bodies or protein aggregates were observed in the skeletal muscle of *neb*^{-/-}*nrap*^{+/-} zebrafish (Fig. 6A and D). Although the 100% reduction of Nrap (*neb*^{-/-}*nrap*^{-/-}) did not restore the sarcomere length or improve sarcomere height, a 50% reduction in Nrap (*neb*^{-/-}*nrap*^{+/-}) resulted in reduced length of sarcomere. However, no changes were observed in the sarcomere height in *neb*^{-/-}*nrap*^{+/-} zebrafish compared with

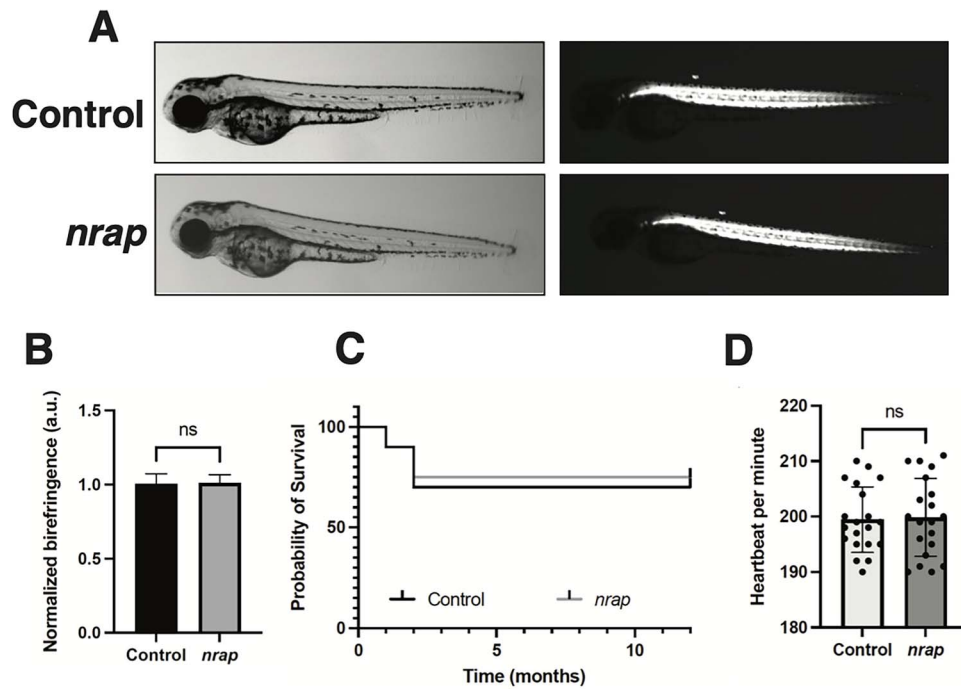


Figure 3. *nrap* mutant zebrafish exhibit normal skeletal and cardiac development and survival. (A) Phenotypic analysis of control and *nrap* mutant zebrafish shows similar morphology at 3 dpf (left). Birefringence analysis (right) and quantification (B) revealing normal skeletal muscle structure in *nrap* mutant zebrafish in comparison to control (3 dpf). (C) Kaplan–Meier Survival curve of the control (+/+) and *nrap* mutant zebrafish analyzed till 12 months. $n = 96$. Zebrafish obtained from three different matings were monitored for survival. (D) Heartbeat analysis of control and *nrap* mutant zebrafish showed no significant differences. $n = 20$ in each group. Five replicates with $n = 8–20$ zebrafish of each genotype were analyzed for every replicate. Data are presented as mean \pm SD. One-way ANOVA with Tukey’s post-hoc test was performed. Non-significant: ns, $**p < 0.01$, $***p < 0.001$.

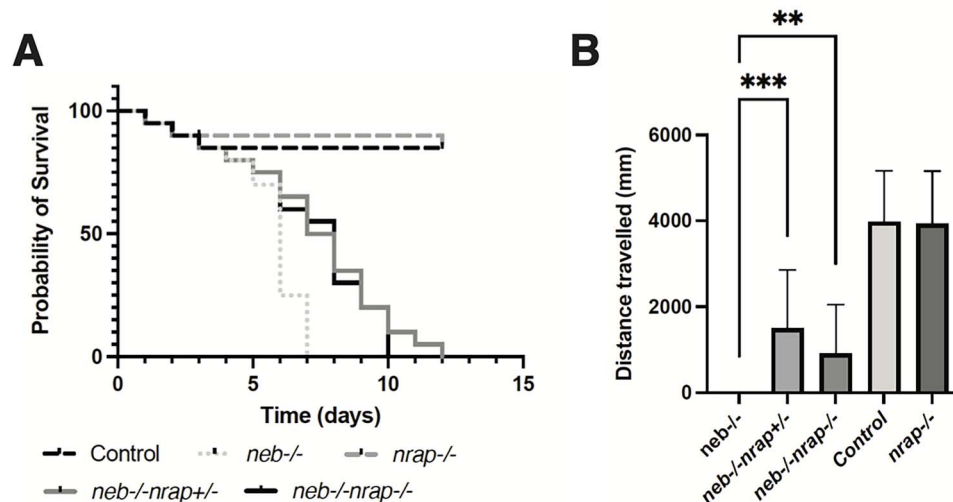


Figure 4. *Nrap* downregulation in nebulin deficiency results in improved survival and skeletal muscle function. (A) Kaplan–Meier’s survival analysis of zebrafish embryonic and larval fish ($n = 96$). (B) Quantification of total swimming distance acquired by automated analysis of zebrafish movement in a multiwall format. $n = 96$ zebrafish were analyzed from four different replicates. Data are presented as mean \pm SD. One-way ANOVA with Tukey’s post-hoc test was performed. Non-significant: ns, $**p < 0.01$, $***p < 0.001$. Scale bar = 50 μ m.

neb-/- larval zebrafish. These data and analyses show that *Nrap* downregulation results in improved sarcomere length, organized sarcomeres and reduction in protein aggregates in skeletal muscle in nebulin deficient skeletal muscle.

Discussion

Identification of genetic disease modifiers is critical to understand the pathological processes and determining potential

therapeutic targets. High amounts of NRAP are detected in the skeletal muscle of patients affected with protein aggregation myopathies (32,34,43). However, the direct link between the role of NRAP in the disease pathology of different myopathies is not clear. Our previous work showed that overexpression of NRAP results in myopathy with structural abnormalities in the skeletal muscle (32). In this study, we have examined NRAP as a disease modifier in the most common form of NM caused by nebulin deficiency. Our studies show that downregulation of *Nrap* in nebulin deficiency

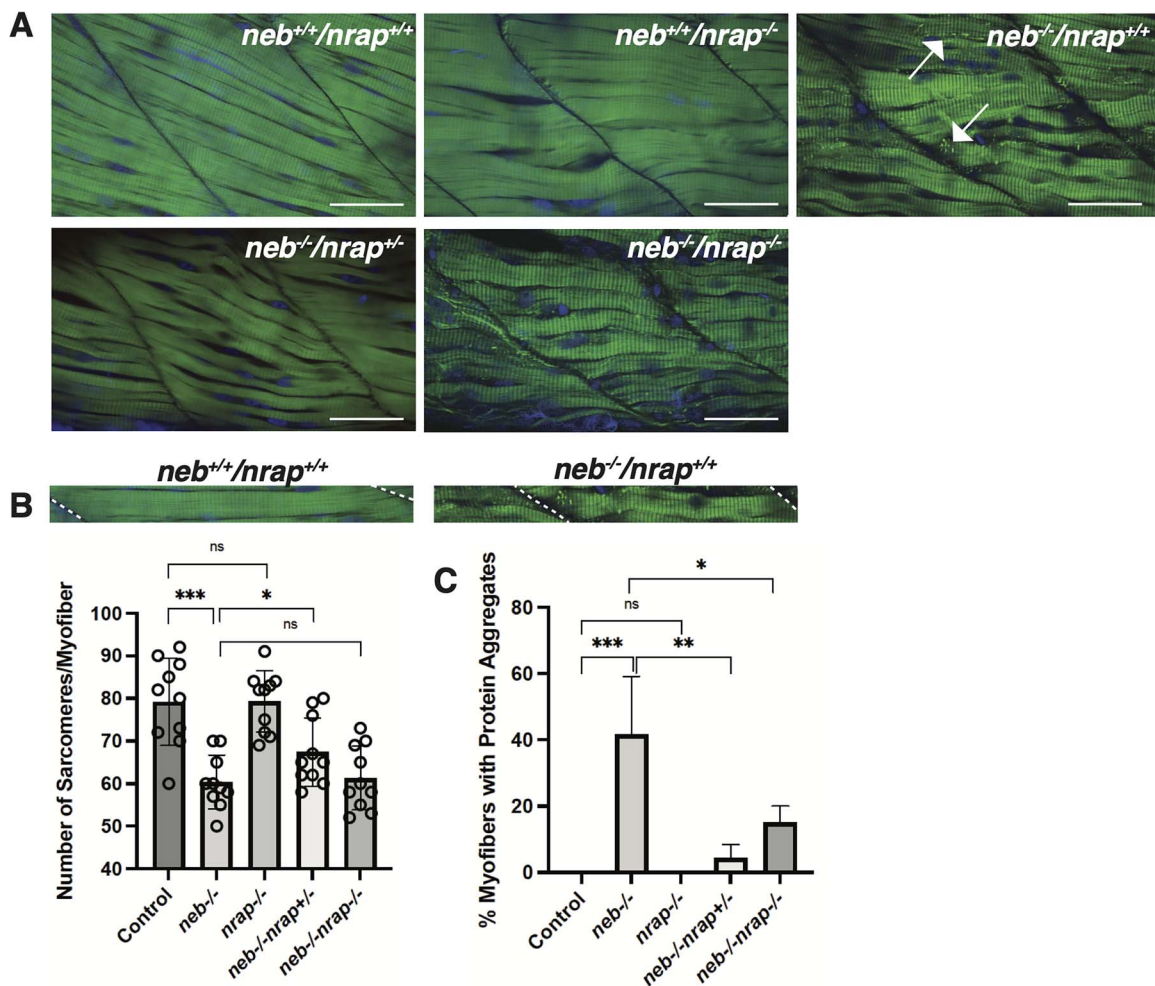


Figure 5. Nrap reduction improves myotome organization in *neb* mutant zebrafish. (A) Wholmount immunofluorescence of control (+/+), *nrap*, *neb*, *neb*^{-/-}*nrap*^{+/-} and *neb*^{-/-}*nrap*^{-/-} zebrafish groups (6 dpf). Maximum intensity projection confocal images showed disorganized myofibers with reduced sarcomere number per myofiber and protein aggregates in *neb* mutant fish. Decreasing Nrap levels in *neb* deficiency improves myotome organization and reduce protein aggregates without affecting sarcomere number per myofiber. (B) Quantification of the number of sarcomeres/myofiber and (C) quantification of myofibers exhibiting phalloidin stained actin protein aggregates. Data are presented as mean \pm SD. One-way ANOVA with Tukey's post-hoc test was performed. Non-significant: ns, ** $p < 0.01$, *** $p < 0.001$. $n = 10$ –20 zebrafish were analyzed in each replicate. Scale bar = 50 μ m.

improves skeletal muscle structure and function and increases survival.

NRAP is a nebulin family member that is expressed in cardiac and skeletal muscle. Our studies in mice and zebrafish identified increased amounts of *Nrap* transcripts and protein in nebulin deficiency. Our previous studies in KLHL41-NM showed that Nrap protein in skeletal muscle is upregulated because of reduced turnover by ubiquitination-mediated proteasomal degradation defects in KLHL41 deficiency. KLHL41 forms a ubiquitination complex with the E3 ubiquitin ligase CUL3 in skeletal muscle to target specific proteins for degradation including NRAP (32). Previous studies in *Neb*^{-/-} mice have shown that KLHL41 is upregulated in nebulin deficiency (36). This is intriguing as increased levels of KLHL41 would imply an increase in NRAP protein degradation in nebulin deficiency by the KLHL41-CUL3 ubiquitination complex (11). Unlike KLHL41, CUL3 E3 ligase is significantly reduced in nebulin deficiency, suggesting impairment in the assembly and/or function of the KLHL41-CUL3 ubiquitination complex and a corresponding accumulation of Nrap in the skeletal muscle (36). In nebulin deficiency, upregulation of *Nrap* at both transcriptional (mRNA) and post-translational (protein)

level suggests different mechanisms may contribute to Nrap upregulation in different genetic forms of myopathies. NRAP is a nebulin family member, and the increase in NRAP levels in nebulin deficiency could be owing to genetic compensation as seen previously in other gene families (44–46). In addition to Nrap upregulation, we also identified mislocalization of Nrap protein in nebulin deficient myofibers in zebrafish. NRAP is normally expressed in developing sarcomeres and is required for premyofibril assembly during skeletal muscle development (40). As myofibers mature, Nrap expression is lost from mature sarcomeres and becomes concentrated near to myotendinous junction in myofibers. However, *neb*^{-/-} mutant myofibers exhibited aberrant and random localization of Nrap protein within the myofibers. Recent scRNA-seq studies in mice have identified a small myonuclei population in skeletal muscle enriched in transcripts for components of premyofibril complex, including NRAP (37). Although the functional significance of this myonuclei population is not clear, these may represent early response myonuclei to target local lesions in myofibers. Previous studies have shown that upon muscle injury, actin binding XIRP proteins are localized to the site of muscle damage independent of the PAX7⁺-dependent repair program (47). Therefore, increased

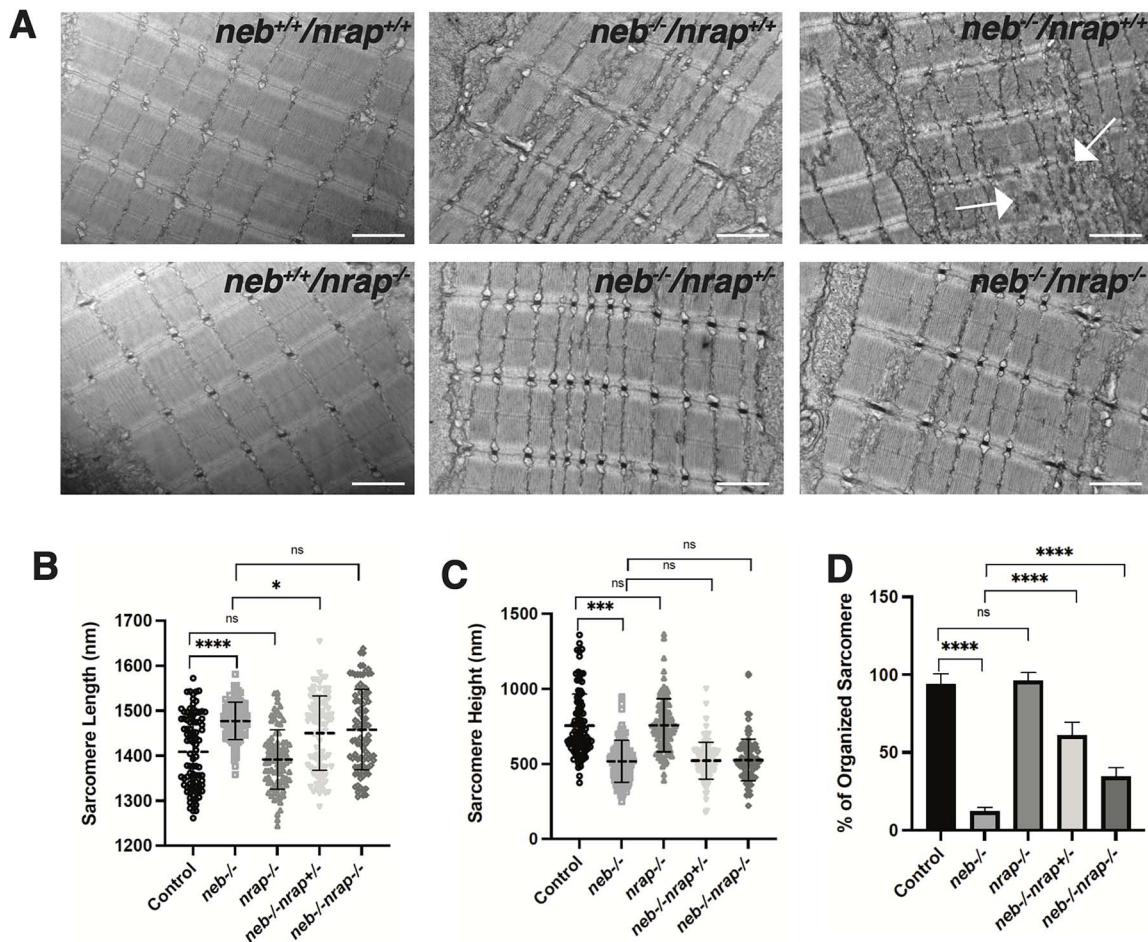


Figure 6. Nrap downregulation improves sarcomere structure in *neb* mutant zebrafish. (A) Ultrastructure examination of control (+/+), *nrap*, *neb*, *neb*^{-/-}*nrap*^{+/-} and *neb*^{-/-}*nrap*^{-/-} zebrafish groups (6 dpf) by transmission electron microscopy showed disorganized and misaligned sarcomeres with electron-dense protein aggregates (arrows) in *neb* mutant fish. Decreasing Nrap levels in *neb* deficiency improve sarcomere organization and reduce protein aggregates. (B)–(C) Quantification of sarcomere length and height, respectively, in different genotypes. (D) Quantification of % of organized sarcomeres. Data are presented as mean ± SD. One-way ANOVA with Tukey's post-hoc test was performed. Non-significant: ns, ***p* < 0.01, ****p* < 0.001. *n* = 3 zebrafish were analyzed from each genotype from two different replicates. Scale bar = 500 uM.

and abnormal localization of Nrap within myofibers could be a compensatory response to myofiber damage observed either in the complete absence of nebulin or in the presence of disease-causing mutant nebulin in NM. However, abnormal sequestration of sarcomeric proteins or lack of myofibrillar proteins that are required for the formation of the mature sarcomere in the disease state, such as nebulin, may prevent further repair of sarcomeres. Our previous studies showed that abnormal expression of NRAP in myofibers results in abnormal sequestration of sarcomeric proteins, resulting in disorganized sarcomeres (32). Nrap downregulation resulted in improved Z-line structures in sarcomeres as well as sarcomere number in nebulin deficiency, suggesting that a decrease in NRAP and protein sequestration may improve the availability of sarcomeric proteins to form normal sarcomeres. Moreover, protein aggregates or nemaline bodies were significantly reduced on *nrap* downregulation in *neb*^{-/-} zebrafish. Although no direct correlation has been found between the number of protein aggregates and disease severity in NM, the presence of sarcomeric protein aggregates may interfere with the sarcomere function. Nrap downregulation significantly improved sarcomere organization and swimming behavior of nebulin mutant zebrafish. Moreover, Nrap downregulation rescued the reduced number of sarcomeres

observed in the series observed in nebulin deficiency. Although this approach did not result in a complete rescue of life span in nebulin deficiency, a significant increase in both life span and skeletal muscle function suggests Nrap downregulation could be therapeutically beneficial to nebulin-NM. Finally, we investigated if the positive effects of *nrap* downregulation in *neb* deficiency are associated with any negative effects of *nrap* reduction in cardiac and skeletal muscle. Nrap mutant zebrafish exhibited normal skeletal muscle, cardiac function and survival, showing *nrap* reduction may not have any detrimental effects in these tissues. Recent studies have shown that biallelic loss of NRAP protein function variants results in low penetrance genetic risk for cardiomyopathy (48,49). However, no abnormalities were reported in skeletal muscle, heterozygous family members or homozygous siblings with the truncating NRAP variant.

We observed better structural and functional outcomes on 50% Nrap downregulation in nebulin deficiency in comparison to a complete absence of Nrap. Therefore, partial reduction of NRAP in nebulin deficient patients may benefit these patients without any detrimental negative effects. Modulation of modifier genes in genetic diseases has shown considerable therapeutic potential in congenital muscle diseases in mice and patient muscle cells

(50–53). Recent studies have also identified small molecule regulators of muscle function in NM. Omecamtiv, mecarbil and levosimendan, which are small molecule regulators of calcium sensitivity and troponin activator CK-2066260 (fiber type II activator) studies in nebulin deficient mice, show an improvement of force generation at submaximal activation levels (54–56). NM caused by defects in a large protein like nebulin is extremely challenging to be targeted by a single therapy. Therefore, the identification of NRAP as a modifier of NM may be beneficial for patients for combination therapy in the future for the complete rescue of skeletal muscle function.

Materials and Methods

Zebrafish lines

Fish were bred and maintained using standard methods as described (57). All procedures were approved by the Brigham and Women's Hospital Animal Care and Use Committee. *neb*^{sa906} and *nrap*^{sa42059} zebrafish lines were obtained from ZIRC. Zebrafish embryonic (0–2 days post fertilization) and larval stages (3–5 dpf) have been defined as described previously (58).

Genotyping assays for *neb*^{sa906} and *nrap*^{sa42059} lines

DNA was extracted from zebrafish larvae or fin clips of adult zebrafish and genotyped by PCR and Sanger sequencing (59). PCR Primer sequences are available in [Supplementary Material, Table S1](#). RT-PCR with Invitrogen TaqMan Custom SNP primers was also used to genotype *neb* or *nrap* fish. Unknown DNA samples were analyzed with wild-type, heterozygous or mutant samples as controls with TaqPath ProAmp Master Mix (Thermo Fisher, #A30865) in a 96-well format. RT-PCR with each probe was performed separately in the following conditions: 3 min at 95°C, 39 cycles of 10 s at 95°C and 30 s at 55°C. Genotypes were successively identified by the Bio-Rad CFX Maestro software using the ratio of FAM to VIC signal.

Birefringence

Muscle birefringence was analyzed as described previously (60). Quantification data were calculated for five posterior somites (numbers 12–16) that exhibited flat orientation in zebrafish. Mean pixel intensity was divided by the skeletal muscle area for each zebrafish birefringence image using ImageJ (National Institutes of Health, Bethesda, MD, USA), a value that was then normalized to WT controls.

Whole mount phalloidin staining

Zebrafish larvae (6–7 days post-fertilization) were fixed in 4% PFA overnight at 4°C, then washed as follows: 2 × 10 min in PBS, 2 × 10 min in PBS-T (0.1% Tween-20), 1 × 60 min in PBS-TR (2% Triton X) and 2 × 5 min in PBS-T. Larval zebrafish were blocked in PBS-T containing 5% goat serum for 1 hour at RT and incubated with phalloidin (1:40, Thermo Fisher Scientific, A12379). Subsequently, larvae were washed for 4 × 15 min in PBS-T, mounted in 3% carboxymethylcellulose and visualized using a Nikon Ti2 spinning disk confocal microscope.

Western blotting

Protein analysis on flash-frozen muscle tissue from mice by Western blotting was performed as previously described (36). NRAP (1:250, HPA037954-25UL, Sigma-Aldrich, St Louis, MO, USA) was used to detect NRAP expression by Western Blot. GAPDH expression was used to normalize other western blots. Secondary

antibodies conjugated with fluorescent dyes with infrared excitation spectra were used for detection. IR western blots were analyzed using Odyssey Infrared Imaging System (Li-Cor Biosciences, NE, USA). Zebrafish larvae at 6–7 dpf were homogenized in buffer containing Tris–Cl (20 mM, pH 7.6), NaCl (50 mM), EDTA (1 mM), NP-40 (0.1%) and complete protease inhibitor cocktail (Roche Applied Sciences, Indianapolis, IN, USA). Following centrifugation at 11 000 g at 4°C for 15 min, protein concentration in supernatants was determined by BCA protein assay (Pierce, Rockford, IL, USA). Proteins were separated by electrophoresis on 4–12% gradient Tris–glycine gels (Invitrogen) and transferred onto polyvinylidene difluoride membrane (Invitrogen). Membranes were blocked in PBS containing 5% casein/0.1% Tween 20 and incubated with either rabbit polyclonal anti NRAP (1:250, HPA037954-25UL, Sigma-Aldrich, St Louis, MO, USA) or mouse monoclonal anti α -tubulin (1:500, T9026-100UL, Sigma-Aldrich) primary antibodies. After washing, membranes were incubated with horseradish peroxidase-conjugated antirabbit (1: 2500, 170–6515) or anti-mouse (1: 5000, 170–6516) IgG secondary antibodies (BioRad, Hercules, CA, USA). Proteins were detected using the SuperSignal chemiluminescent substrate kit (Pierce).

Myofiber isolation and immunofluorescence

Myofibers were isolated from control or *neb*^{–/–} larval zebrafish (6–7 dpf) as described previously (61). Fixed cells were blocked in 10% goat serum/0.3% Triton, incubated in primary antibody overnight at 4°C, washed in PBS, incubated in secondary antibody for 1 h at room temperature (RT), washed in PBS, then mounted with Vectashield Mounting Medium (Vector Laboratories, Burlingame, CA, USA). Primary antibodies used were rabbit polyclonal anti NRAP (1: 100, HPA037954, Sigma-Aldrich), mouse monoclonal anti sarcomeric α -actinin (1: 100, A7732, Sigma) and FITC-phalloidin (1:40, Thermo Fisher Scientific, A12379). After washing in PBS several times, samples were incubated with anti-mouse Alexa Fluor (1: 100, A-11005) secondary antibody (ThermoFisher Scientific). Imaging was performed using a Nikon Ti2 spinning disk confocal microscope.

RT-PCR assay

To detect *nrap* mRNA expression in zebrafish, RNA was prepared from control or *neb* knockout zebrafish (6 dpf) using Rnaeasy fibrous tissue mini kit (Qiagen) according to the manufacturer's instructions. cDNAs were synthesized from 1 μ g of total RNA using Superscript II reverse transcriptase (Thermo Fisher Scientific) and random hexamers.

Zebrafish locomotion assay

Zebrafish swimming behavior was quantified by using the Zantiks MWP automated tracking system (Zantiks Ltd, Cambridge, UK). Larval zebrafish were placed individually into each well of a 24-well plate and their swimming behavior was recorded for 50 min (10 min light, 10 min dark, 10 min light, 10 min dark, 10 min light, end). Four independent blind trials were performed, and the total distance and cumulative duration of the movement were recorded. Reported values reflect data from 96 larval fish in a single replicate.

Electron microscopy

6–7 dpf zebrafish embryos were fixed in formaldehyde–glutaraldehyde–picric acid in cacodylate buffer overnight at 4°C, followed by osmication and uranyl acetate staining. Subsequently, embryos were dehydrated in a series of ethanol washes and embedded in TAAB Epon (Marivac Ltd, Halifax, NS, Canada).

Sections (95 nm) were cut with a Leica UltraCut microtome, picked up on 100-mm Formvar-coated copper grids and stained with 0.2% lead citrate. To check the orientation of the samples, thin sections of the muscle tissue were viewed by light microscopy before performing the electron microscopy. Samples with oblique orientations were discarded. Sections were viewed and imaged using a JEOL 1200EX transmission electron microscope at the Harvard Medical School Electron Microscopy Core.

Quantification and statistical analysis

All samples were blinded till final analyses and statistical analyses were performed using GraphPad Prism9.

Supplementary Material

Supplementary Material is available at HMG online.

Acknowledgements

The authors also thank Praju Vikas Anekal of the MicroN core facility for help with imaging data analysis and Louis Trakimas at the electron microscopy core for assistance with sample preparation and data acquisition at Harvard Medical School.

Conflict of Interest statement. None declared.

Funding

National Institutes of Health (R56AR077017 to V.A.G.); A Foundation Building Strength grant and Innovation Evergreen Fund Award (to V.A.G.); National Institutes of Health (R01 AR053897 to H.G.).

References

- Laitila, J. and Wallgren-Pettersson, C. (2021) Recent advances in nemaline myopathy. *Neuromuscul. Disord.*, **31**, 955–967.
- Gonorazky, H.D., Bonnemann, C.G. and Dowling, J.J. (2018) The genetics of congenital myopathies. *Handb. Clin. Neurol.*, **148**, 549–564.
- Nowak, K.J., Wattanasirichaigoon, D., Goebel, H.H., Wilce, M., Pelin, K., Donner, K., Jacob, R.L., Hubner, C., Oexle, K., Anderson, J.R. et al. (1999) Mutations in the skeletal muscle alpha-actin gene in patients with actin myopathy and nemaline myopathy. *Nat. Genet.*, **23**, 208–212.
- Pelin, K., Hilpela, P., Donner, K., Sewry, C., Akkari, P.A., Wilton, S.D., Wattanasirichaigoon, D., Bang, M.L., Centner, T., Hanefeld, F. et al. (1999) Mutations in the nebulin gene associated with autosomal recessive nemaline myopathy. *Proc. Natl. Acad. Sci. U. S. A.*, **96**, 2305–2310.
- Laing, N.G., Wilton, S.D., Akkari, P.A., Dorosz, S., Boundy, K., Kneebone, C., Blumbergs, P., White, S., Watkins, H. and Love, D.R. (1995) A mutation in the alpha tropomyosin gene TPM3 associated with autosomal dominant nemaline myopathy NEM1. *Nat. Genet.*, **10**, 249.
- Donner, K., Ollikainen, M., Ridanpaa, M., Christen, H.J., Goebel, H.H., de Visser, M., Pelin, K. and Wallgren-Pettersson, C. (2002) Mutations in the beta-tropomyosin (TPM2) gene—a rare cause of nemaline myopathy. *Neuromuscular disorders: NMD*, **12**, 151–158.
- Lehtokari, V.L., Kiiski, K., Sandaradura, S.A., Laporte, J., Repo, P., Frey, J.A., Donner, K., Marttila, M., Saunders, C., Barth, P.G. et al. (2014) Mutation update: the spectra of nebulin variants and associated myopathies. *Hum. Mutat.*, **35**, 1418–1426.
- Johnston, J.J., Kelley, R.I., Crawford, T.O., Morton, D.H., Agarwala, R., Koch, T., Schaffer, A.A., Francomano, C.A. and Biesecker, L.G. (2000) A novel nemaline myopathy in the Amish caused by a mutation in troponin T1. *Am. J. Hum. Genet.*, **67**, 814–821.
- Sandaradura, S.A., Bournazos, A., Mallawaarachchi, A., Cummings, B.B., Waddell, L.B., Jones, K.J., Troedson, C., Sudarsanam, A., Nash, B.M., Peters, G.B. et al. (2018) Nemaline myopathy and distal arthrogryposis associated with an autosomal recessive TNNT3 splice variant. *Hum. Mutat.*, **39**, 383–388.
- Ravenscroft, G., Miyatake, S., Lehtokari, V.L., Todd, E.J., Vornanen, P., Yau, K.S., Hayashi, Y.K., Miyake, N., Tsurusaki, Y., Doi, H. et al. (2013) Mutations in KLHL40 are a frequent cause of severe autosomal-recessive nemaline myopathy. *Am. J. Hum. Genet.*, **93**, 6–18.
- Gupta, V.A., Ravenscroft, G., Shaheen, R., Todd, E.J., Swanson, L.C., Shiina, M., Ogata, K., Hsu, C., Clarke, N.F., Darras, B.T. et al. (2013) Identification of KLHL41 mutations implicates BTB-Kelch-mediated ubiquitination as an alternate pathway to Myofibrillar disruption in nemaline myopathy. *Am. J. Hum. Genet.*, **93**, 1108–1117.
- Yuen, M., Sandaradura, S.A., Dowling, J.J., Kostyukova, A.S., Moroz, N., Quinlan, K.G., Lehtokari, V.L., Ravenscroft, G., Todd, E.J., Ceyhan-Birsoy, O. et al. (2014) Leiomodin-3 dysfunction results in thin filament disorganization and nemaline myopathy. *J. Clin. Invest.*, **124**, 4693–4708.
- Agrawal, P.B., Greenleaf, R.S., Tomczak, K.K., Lehtokari, V.L., Wallgren-Pettersson, C., Wallefeld, W., Laing, N.G., Darras, B.T., Maciver, S.K., Dormitzer, P.R. et al. (2007) Nemaline myopathy with minicores caused by mutation of the CFL2 gene encoding the skeletal muscle actin-binding protein, cofilin-2. *Am. J. Hum. Genet.*, **80**, 162–167.
- Amburgey, K., Acker, M., Saeed, S., Amin, R., Beggs, A.H., Bönnemann, C.G., Brudno, M., Constantinescu, A., Dastgir, J., Diallo, M. et al. (2021) A cross-sectional study of nemaline myopathy. *Neurology*, **96**, e1425–e1436.
- Feingold-Zadok, M., Chitayat, D., Chong, K., Injeyan, M., Shannon, P., Chapmann, D., Maymon, R., Pillar, N. and Reish, O. (2017) Mutations in the NEB gene cause fetal akinesia/arthrogryposis multiplex congenita. *Prenat. Diagn.*, **37**, 144–150.
- Lehtokari, V.L., Greenleaf, R.S., DeChene, E.T., Kellinsalmi, M., Pelin, K., Laing, N.G., Beggs, A.H. and Wallgren-Pettersson, C. (2009) The exon 55 deletion in the nebulin gene—one single founder mutation with world-wide occurrence. *Neuromuscul. Disord.*, **19**, 179–181.
- Donner, K., Sandbacka, M., Lehtokari, V.L., Wallgren-Pettersson, C. and Pelin, K. (2004) Complete genomic structure of the human nebulin gene and identification of alternatively spliced transcripts. *Eur. J. Hum. Genet.*, **12**, 744–751.
- Buck, D., Hudson, B.D., Ottenheim, C.A., Labeit, S. and Granzier, H. (2010) Differential splicing of the large sarcomeric protein nebulin during skeletal muscle development. *J. Struct. Biol.*, **170**, 325–333.
- Labeit, S. and Kolmerer, B. (1995) The complete primary structure of human nebulin and its correlation to muscle structure. *J. Mol. Biol.*, **248**, 308–315.
- Pelin, K. and Wallgren-Pettersson, C. (2008) Nebulin—a giant chameleon. *Adv. Exp. Med. Biol.*, **642**, 28–39.
- Laitila, J., Hanif, M., Paetau, A., Hujanen, S., Keto, J., Somervuo, P., Huovinen, S., Udd, B., Wallgren-Pettersson, C., Auvinen, P., Hackman, P. and Pelin, K. (2012) Expression of multiple nebulin isoforms in human skeletal muscle and brain. *Muscle Nerve*, **46**, 730–737.

22. Björklund, A.K., Light, S., Sagit, R. and Elofsson, A. (2010) Nebulin: a study of protein repeat evolution. *J. Mol. Biol.*, **402**, 38–51.
23. Bang, M.L., Li, X., Littlefield, R., Bremner, S., Thor, A., Knowlton, K.U., Lieber, R.L. and Chen, J. (2006) Nebulin-deficient mice exhibit shorter thin filament lengths and reduced contractile function in skeletal muscle. *J. Cell Biol.*, **173**, 905–916.
24. Witt, C.C., Burkart, C., Labeit, D., McNabb, M., Wu, Y., Granzier, H. and Labeit, S. (2006) Nebulin regulates thin filament length, contractility, and Z-disk structure in vivo. *EMBO J.*, **25**, 3843–3855.
25. Tonino, P., Pappas, C.T., Hudson, B.D., Labeit, S., Gregorio, C.C. and Granzier, H. (2010) Reduced myofibrillar connectivity and increased Z-disk width in nebulin-deficient skeletal muscle. *J. Cell Sci.*, **123**, 384–391.
26. Lindqvist, J., Ma, W., Li, F., Hernandez, Y., Kolb, J., Kiss, B., Tonino, P., van der Pijl, R., Karimi, E., Gong, H. et al. (2020) Triggering typical nemaline myopathy with compound heterozygous nebulin mutations reveals myofilament structural changes as pathomechanism. *Nat. Commun.*, **11**, 2699.
27. Li, F., Kolb, J., Crudele, J., Tonino, P., Hourani, Z., Smith, J.E., 3rd, Chamberlain, J.S. and Granzier, H. (2020) Expressing a Z-disk nebulin fragment in nebulin-deficient mouse muscle: effects on muscle structure and function. *Skelet. Muscle*, **10**, 2.
28. Li, F., Barton, E.R. and Granzier, H. (2019) Deleting nebulin's C-terminus reveals its importance to sarcomeric structure and function and is sufficient to invoke nemaline myopathy. *Hum. Mol. Genet.*, **28**, 1709–1725.
29. Joureau, B., de Winter, J.M., Stam, K., Granzier, H. and Ottenheijm, C.A. (2017) Muscle weakness in respiratory and peripheral skeletal muscles in a mouse model for nebulin-based nemaline myopathy. *Neuromuscul. Disord.*, **27**, 83–89.
30. Laitila, J.M., McNamara, E.L., Wingate, C.D., Goulee, H., Ross, J.A., Taylor, R.L., van der Pijl, R., Griffiths, L.M., Harries, R., Ravenscroft, G. et al. (2020) Nebulin nemaline myopathy recapitulated in a compound heterozygous mouse model with both a missense and a nonsense mutation in neb. *Acta Neuropathol. Commun.*, **8**, 18.
31. Telfer, W.R., Nelson, D.D., Waugh, T., Brooks, S.V. and Dowling, J.J. (2012) Neb: a zebrafish model of nemaline myopathy due to nebulin mutation. *Dis. Model. Mech.*, **5**, 389–396.
32. Jirka, C., Pak, J.H., Grosogeat, C.A., Marchetti, M.M. and Gupta, V.A. (2019) Dysregulation of NRAP degradation by KLHL41 contributes to pathophysiology in nemaline myopathy. *Hum. Mol. Genet.*, **28**, 2549–2560.
33. Mohiddin, S.A., Lu, S., Cardoso, J.P., Carroll, S., Jha, S., Horowitz, R. and Fananapazir, L. (2003) Genomic organization, alternative splicing, and expression of human and mouse N-RAP, a nebulin-related LIM protein of striated muscle. *Cell Motil. Cytoskeleton*, **55**, 200–212.
34. Feldkirchner, S., Schessl, J., Muller, S., Schoser, B. and Hanisch, F.G. (2012) Patient-specific protein aggregates in myofibrillar myopathies: laser microdissection and differential proteomics for identification of plaque components. *Proteomics*, **12**, 3598–3609.
35. Sztal, T.E., McKaige, E.A., Williams, C., Oorschot, V., Ramm, G. and Bryson-Richardson, R.J. (2018) Testing of therapies in a novel nebulin nemaline myopathy model demonstrate a lack of efficacy. *Acta Neuropathol. Commun.*, **6**, 40.
36. Li, F., Buck, D., De Winter, J., Kolb, J., Meng, H., Birch, C., Slater, R., Escobar, Y.N., Smith, J.E., 3rd, Yang, L. et al. (2015) Nebulin deficiency in adult muscle causes sarcomere defects and muscle-type-dependent changes in trophicity: novel insights in nemaline myopathy. *Hum. Mol. Genet.*, **24**, 5219–5233.
37. Petrany, M.J., Swoboda, C.O., Sun, C., Chetal, K., Chen, X., Weirauch, M.T., Salomonis, N. and Millay, D.P. (2020) Single-nucleus RNA-seq identifies transcriptional heterogeneity in multinucleated skeletal myofibers. *Nat. Commun.*, **11**, 6374.
38. Wen, Y., Englund, D.A., Peck, B.D., Murach, K.A., McCarthy, J.J. and Peterson, C.A. (2021) Myonuclear transcriptional dynamics in response to exercise following satellite cell depletion. *iScience*, **24**, 102838.
39. Karlsen, A., Gonzalez-Franquesa, A., Jakobsen, J.R., Krogsgaard, M.R., Koch, M., Kjaer, M., Schiaffino, S., Mackey, A.L. and Deshmukh, A.S. (2022) The proteomic profile of the human myotendinous junction. *iScience*, **25**, 103836.
40. Lu, S., Borst, D.E. and Horowitz, R. (2008) Expression and alternative splicing of N-RAP during mouse skeletal muscle development. *Cell Motil. Cytoskeleton*, **65**, 945–954.
41. Lawlor, M.W., Ottenheijm, C.A., Lehtokari, V.L., Cho, K., Pelin, K., Wallgren-Pettersson, C., Granzier, H. and Beggs, A.H. (2011) Novel mutations in NEB cause abnormal nebulin expression and markedly impaired muscle force generation in severe nemaline myopathy. *Skelet. Muscle*, **1**, 23.
42. Smith, L.R., Lee, K.S., Ward, S.R., Chambers, H.G. and Lieber, R.L. (2011) Hamstring contractures in children with spastic cerebral palsy result from a stiffer extracellular matrix and increased in vivo sarcomere length. *J. Physiol.*, **589**, 2625–2639.
43. Kley, R.A., Maerkens, A., Leber, Y., Theis, V., Schreiner, A., van der Ven, P.F., Uszkoreit, J., Stephan, C., Eulitz, S., Euler, N. et al. (2013) A combined laser microdissection and mass spectrometry approach reveals new disease relevant proteins accumulating in aggregates of filaminopathy patients. *Mol. Cell. Proteomics*, **12**, 215–227.
44. Sztal, T.E., McKaige, E.A., Williams, C., Ruparella, A.A. and Bryson-Richardson, R.J. (2018) Genetic compensation triggered by actin mutation prevents the muscle damage caused by loss of actin protein. *PLoS Genet.*, **14**, e1007212.
45. El-Brolosy, M.A., Kontarakis, Z., Rossi, A., Kuenne, C., Günther, S., Fukuda, N., Kikhi, K., Boezio, G.L.M., Takacs, C.M., Lai, S.L. et al. (2019) Genetic compensation triggered by mutant mRNA degradation. *Nature*, **568**, 193–197.
46. Diofano, F., Weinmann, K., Schneider, I., Thiessen, K.D., Rotbauer, W. and Just, S. (2020) Genetic compensation prevents myopathy and heart failure in an in vivo model of Bag3 deficiency. *PLoS Genet.*, **16**, e1009088.
47. Otten, C., van der Ven, P.F., Lewrenz, I., Paul, S., Steinhagen, A., Busch-Nentwich, E., Eichhorst, J., Wiesner, B., Stemple, D., Strähle, U., Fürst, D.O. and Abdelilah-Seyfried, S. (2012) Xirp proteins mark injured skeletal muscle in zebrafish. *PLoS One*, **7**, e31041.
48. Truszkowska, G.T., Bilińska, Z.T., Muchowicz, A., Pollak, A., Biernacka, A., Kozar-Kamińska, K., Stawiński, P., Gasperowicz, P., Kosińska, J., Zieliński, T. and Płoski, R. (2017) Homozygous truncating mutation in NRAP gene identified by whole exome sequencing in a patient with dilated cardiomyopathy. *Sci. Rep.*, **7**, 3362.
49. Koskenvuo, J.W., Saarinen, I., Ahonen, S., Tommiska, J., Weckström, S., Seppälä, E.H., Tuupainen, S., Kangas-Kontio, T., Schleit, J., Heliö, K. et al. (2021) Biallelic loss-of-function in NRAP is a cause of recessive dilated cardiomyopathy. *PLoS One*, **16**, e0245681.
50. Silva-Rojas, R., Pérez-Guàrdia, L., Lafabrie, E., Moulart, D., Laporte, J. and Böhm, J. (2022) Silencing of the ca(2+) channel ORAI1 improves the multi-systemic phenotype of tubular aggregate myopathy (TAM) and Stormorken syndrome (STRMK)

- in mice. *Int. J. Mol. Sci.*, **23**, 6968. <https://doi.org/10.3390/ijms23136968>
51. Silva-Rojas, R., Nattarayan, V., Jaque-Fernandez, F., Gomez-Oca, R., Menuet, A., Reiss, D., Goret, M., Messaddeq, N., Lionello, V.M., Kretz, C. et al. (2022) Mice with muscle-specific deletion of Bin1 recapitulate centronuclear myopathy and acute downregulation of dynamin 2 improves their phenotypes. *Mol. Ther.*, **30**, 868–880.
 52. Cowling, B.S., Chevremont, T., Prokic, I., Kretz, C., Ferry, A., Coirault, C., Koutsopoulos, O., Laugel, V., Romero, N.B. and Laporte, J. (2014) Reducing dynamin 2 expression rescues X-linked centronuclear myopathy. *J. Clin. Invest.*, **124**, 1350–1363.
 53. Kemaladewi, D.U., Bassi, P.S., Erwood, S., Al-Basha, D., Gawlik, K.I., Lindsay, K., Hyatt, E., Kember, R., Place, K.M., Marks, R.M. et al. (2019) A mutation-independent approach for muscular dystrophy via upregulation of a modifier gene. *Nature*, **572**, 125–130.
 54. Lindqvist, J., Lee, E.J., Karimi, E., Kolb, J. and Granzier, H. (2019) Omecamtiv mecarbil lowers the contractile deficit in a mouse model of nebulin-based nemaline myopathy. *PLoS One*, **14**, e0224467.
 55. de Winter, J.M., Joureau, B., Sequeira, V., Clarke, N.F., van der Velden, J., Stienen, G.J., Granzier, H., Beggs, A.H. and Ottenheijm, C.A. (2015) Effect of levosimendan on the contractility of muscle fibers from nemaline myopathy patients with mutations in the nebulin gene. *Skelet. Muscle*, **5**, 12.
 56. de Winter, J.M., Buck, D., Hidalgo, C., Jasper, J.R., Malik, F.I., Clarke, N.F., Stienen, G.J., Lawlor, M.W., Beggs, A.H., Ottenheijm, C.A. and Granzier, H. (2013) Troponin activator augments muscle force in nemaline myopathy patients with nebulin mutations. *J. Med. Genet.*, **50**, 383–392.
 57. Westerfield, M. (2000) *The Zebrafish Book: A Guide for the Laboratory Use of Zebrafish (Danio Rerio)*. Institute of Neuroscience, University of Oregon.
 58. Kimmel, C.B., Ballard, W.W., Kimmel, S.R., Ullmann, B. and Schilling, T.F. (1995) Stages of embryonic development of the zebrafish. *Dev. Dyn.*, **203**, 253–310.
 59. Bennett, A.H., O'Donohue, M.F., Gundry, S.R., Chan, A.T., Widrick, J., Draper, I., Chakraborty, A., Zhou, Y., Zon, L.I., Gleizes, P.E. et al. (2018) RNA helicase, DDX27 regulates skeletal muscle growth and regeneration by modulation of translational processes. *PLoS Genet.*, **14**, e1007226.
 60. Smith, L.L., Beggs, A.H. and Gupta, V.A. (2013) Analysis of skeletal muscle defects in larval zebrafish by birefringence and touch-evoked escape response assays. *J. Vis. Exp.*, **82**, e50925.
 61. Horstick, E.J., Gibbs, E.M., Li, X., Davidson, A.E. and Dowling, J.J. (2013) Analysis of embryonic and larval zebrafish skeletal myofibers from dissociated preparations. *J. Vis. Exp.*, **81**, e50259.